

CRYOGENIC SUPPORT THERMAL PERFORMANCE MEASUREMENTS

J.D. Gonczy, W.N. Boroski, T.H. Nicol, R.C. Niemann,
J.G. Otavka, and M.K. Ruschman

Fermi National Accelerator Laboratory
Batavia, Illinois

ABSTRACT

The stringent refrigeration requirements of the Superconducting Super Collider (SSC) and the premium nature of radial space in the SSC cryostat have led to the development of a reentrant tube cryogenic support. Thermal shrink fitting techniques are used to assemble the support. The thermal performance of two cryogenic support models is presented. The geometry of each model, its instrumentation, and experimental test arrangement in a Heat Leak Test Facility are described. Heat leak and temperature profile measurements made with a primary heat intercept temperature controlled between 10 K and 40 K are presented. Heat leak values to 4.5 K were measured by means of a heatmeter. Heat leak values to the primary and secondary heat intercepts were derived using the measured temperature profiles and component material properties. Presented are thermal performance measurements of copper cable connections used to heat sink the primary and secondary heat intercepts to their respective thermal radiation shields. Temperature measurements also were made on identical model supports installed in a full length (17.5 meters long) SSC dipole magnet cryostat thermal model. The thermal performance of the cryogenic supports for the two measurements is compared.

INTRODUCTION

The SSC cryostat development program has resulted in an innovative design for the main structural support member for the SSC magnet cold mass, and the primary and secondary thermal radiation shields.

The Compact Cryogenic Support (CCS) shown in Fig. 1 employs metallic end and heat intercept connections which are securely joined to composite tubes by the clamping pressure generated from designed dimensional interferences between components at the joint locations. Thermal shrink fitting techniques are used to assemble the cryogenic support. The shrink fitted joint provides a tightly clamped connection between the composite tube and the metallic components, and results in a support that maintains its structural integrity for load conditions in tension, compression, bending, and torsion for thermal cycles between 300 K and 4.5 K.

By proper selection of metallic materials, e.g., stainless steel for the inner disc and aluminum for the outer ring, a shrink fitted junction becomes stronger as it becomes colder due to the added clamping afforded by the differential thermal contraction of the junction components. Selection of the composite material for the tubular elements of the CCS is determined by concurrent consideration of stress, deflection, heat leak, creep, and installation geometry. The tubular material must allow for the development of flexure and torsional stiffness while maintaining a small cross-sectional area that is required to limit conduction heat leak.

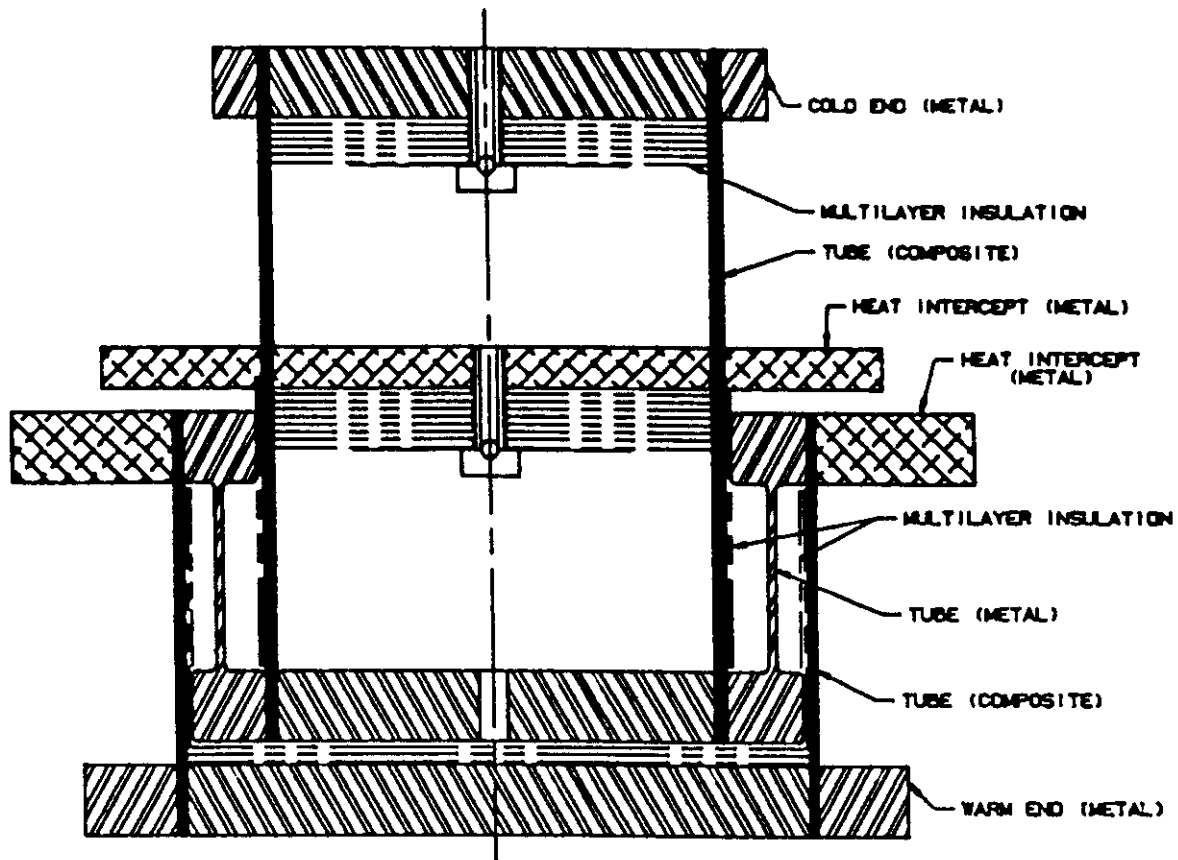


Fig. 1. Compact cryogenic support cross-section.

Also by its nature, a CCS is subject to internal thermal radiation. Internal radiation can significantly affect the thermal performance of the support and must be controlled. Effective control can be achieved by use of multilayer insulation internal to the CCS structure.

As the SSC support requirements became better defined, and the understanding of the structural and thermal performances of the support known, a more substantial CCS was developed, and the earlier model was replaced.^{1,2} Structural and thermal evaluation of the Compact Cryogenic Support continues as working models of the design are optimized.³

COMPACT CRYOGENIC SUPPORT MODEL GEOMETRY

The 4x5 CCS and the 5x7 CCS are designated by the diameters (measured in inches) of the innermost and outermost composite tube elements. The material comprising the composite tubes in the 4x5 CCS model is G-10CR. In the 5x7 CCS, G-11CR is used. The wall thickness of the composite tubes in both models is 1.58 mm.

In each model, a stainless steel middle tubular element bridges the outer and inner composite tubes and accomplishes the reentrance of the conductive heat path within the outer tube, thereby adding length to the path without compromising axial height. The assembled height of each model is 213 mm.

The two models are identical in concept, differing in construction primarily in the size of their corresponding components, and with the 5x7 CCS model having a change in the shape of the stainless steel tubular element.

By design, the CCS has four distinct temperature stations which are defined by the CCS thermal connections. They include a 300 K connection to the room temperature vacuum vessel, an 80 K outer shield support and heat intercept connection, a 20 K inner shield support and heat intercept connection, and a connection to the 4.5 K magnet cold mass.

Multilayer insulation (MLI) internal to the CCS is used to limit radiant heat transfer between components. Radial heat transfer, i.e., radiation between the outer composite tube and the stainless steel middle tube, and between the stainless steel middle tube and the inner composite tube is reduced by MLI spiral wrapped on the corresponding cold areas of temperature boundary surfaces. Thermal radiation in the axial direction is controlled by wafers of MLI secured to the metal discs by tubular G-10 fasteners which allow evacuation of the annular space of the inner composite tube.

THERMAL PERFORMANCE EVALUATIONS IN THE HEAT LEAK TEST FACILITY

CCS temperature profile and heat leak measurements were performed in the Heat Leak Test Facility (HLTF).⁴ Figure 2 illustrates the HLTF and shows the test geometry for the thermal evaluation of the 5x7 CCS with a cold mass slide connection.⁵

The HLTF provides corresponding thermal connections to the CCS temperature stations, and also provides the capability for controlling the inner shield connection at a temperature between 10 K and 40 K. Copper heat sink straps on the CCS heat intercepts are used to thermally anchor the intercepts to their appropriate HLTF thermal connection.

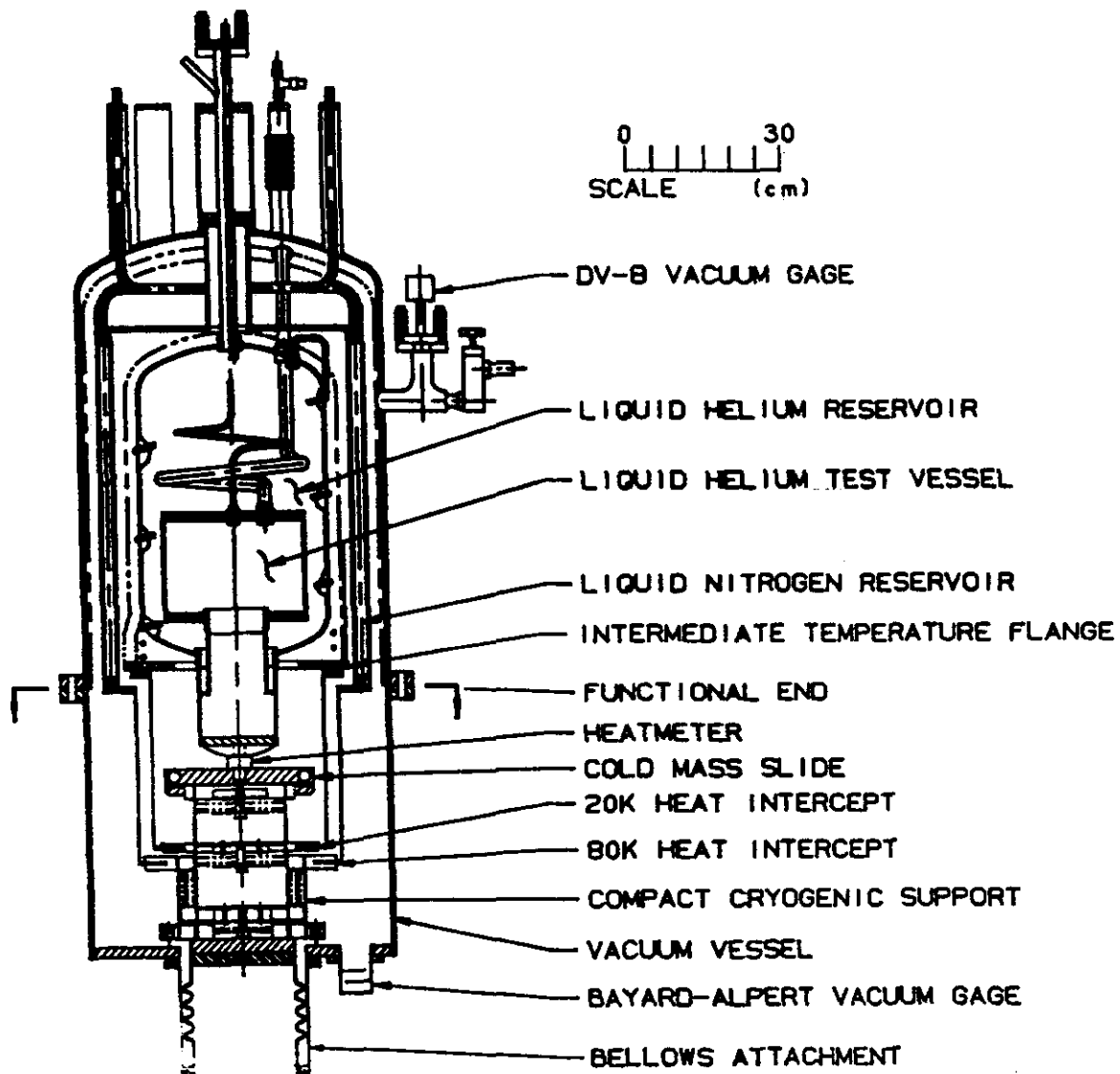


Fig. 2 Heat leak test facility for CCS thermal performance measurements

Carbon resistors are used to monitor HLTF temperatures near 4.5 K; platinum resistance temperature detectors (RTDs) and cryogenic linear temperature sensors (CLTS) are used at temperatures near 80 K.⁶ A four lead-wire system is employed for the sensors. The sensors are connected in series with a constant current source whose polarity is manually controlled. A current of 10 μ A is used for measurements near 4.5 K. For increased sensitivity, 100 μ A is used for temperatures near 80 K. Sensor potential leads are connected to a high impedance data logger.

A bellows attachment to the HLTF vacuum vessel provides an effective load, due to atmospheric pressure, of approximately 273 kg on the CCS test geometry, and allows for thermal motion of the CCS during thermal cycles.

Insulating vacuum in the Heat Leak Test Facility is initiated by a turbomolecular pumping station. System vacuum is monitored by a Bayard-Alpert ionization gage and controller and is recorded by the data acquisition data logger.

The primary method of determining heat leak in the HLTF is by measurement using a heatmeter.⁷ The heatmeter employs a thermally resistive reference section which is sandwiched between thermally conductive ends. For measurements to helium temperatures, a pair of carbon resistors sense the temperature across the reference section. For measurements to 80 K, platinum resistors are used. A calibration heater is located at the warm end of the heatmeter. Calibration of the heatmeter is accomplished by equating the temperature difference across the reference section to the value of heat flow through the heatmeter as generated by the calibration heater. Heatmeter calibration was performed at liquid nitrogen and liquid helium temperatures for ranges of 0 - 3.0 watts to 80 K, and 0 - 0.250 watt to 4.5 K.

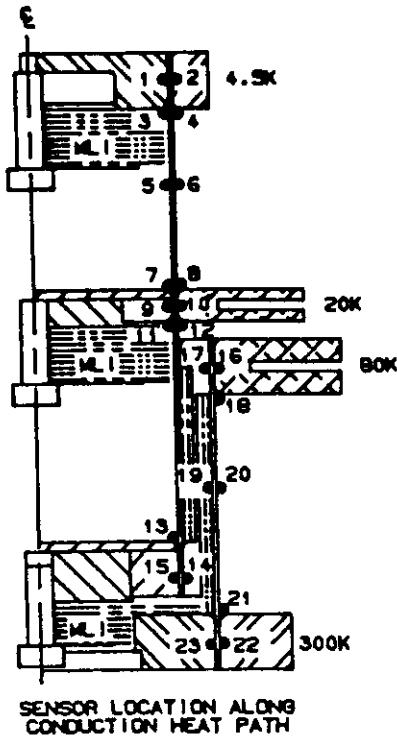
4x5 CCS TEST INSTRUMENTATION AND THERMAL PERFORMANCE RESULTS

The installation geometry of the 4x5 CCS in the HLTF was similar to that shown in Fig. 2, but without the slide attachment, i.e., the heatmeter was connected directly to the 4x5 CCS. The 4x5 CCS was instrumented with 23 temperature sensors which included carbon resistors, platinum RTDs and copper-constantan thermocouples. The sensors were located along the conductive heat path to 4.5 K.

Thermal measurements on the CCS were made with the primary heat intercept controlled at different steady state temperature levels between 10 K and 40 K. The temperature profiles generated by the results of these measurements are listed in Table 1. Subsequent to the measurements in the HLTF, all CCS data recorded by the HLTF data logger was converted for use as computer input. Data recorded in the HLTF was then processed in the same manner as data obtained on CCS performance measurements using a computerized data acquisition system and done in a full length SSC magnet cryostat thermal model.⁸

Graphic representation of 4x5 CCS temperatures during LN₂ cooldown in the HLTF is illustrated in Fig. 3. Figure 3a shows temperatures at the shrink fitted junction of the 20 K heat intercept. The aluminum disc (#9) located inside the inner composite tube is cooled by thermal conduction along the tube length, and also by conduction through the tube wall to the aluminum heat intercept ring (#10). The closeness with which the component temperatures track each other illustrates that the clamping force at a shrink fitted junction is relatively constant for thermal excursions imposed on the junction. Similarly, Fig. 3b shows temperatures of the 80 K lower disc (#15) and the 80 K heat intercept ring (#16). Temperature tracking by the components is through two shrink fitted junctions and includes the thermal impedance of the stainless tube.

Table 1. 4x5 CCS Temperature Profile Measurements



4x5 CCS TEMPERATURE PROFILE MEASUREMENTS (K)						
SENSOR NUMBER	SENSOR TYPE	DESIGN TEMP. (K)	INTERCEPT TEMPERATURE			
			10K	20K	30K	40K
1	CARBON RES.	4.5	5.3	6.0	7.0	9.4
2	CARBON RES.	4.5	5.4	6.0	8.1	9.7
3	CARBON RES.	4.8	5.4	6.9	8.1	9.7
4	CARBON RES.	4.8	5.6	7.7	8.3	11.6
5	CARBON RES.	13.6	8.2	14.7	19.8	27.5
6	CARBON RES.	13.8	8.4	15.4	21.1	29.6
7	CARBON RES.	20.0	8.7	15.4	19.4	24.0
8	CARBON RES.	20.0	11.0	24.3	35.1	49.8
9	CARBON RES.	20.0	10.1	21.2	29.2	40.8
10	CARBON RES.	20.0	10.8	20.8	28.8	40.1
11	CARBON RES.	20.0	13.8	25.1	34.2	46.7
12	CARBON RES.	20.0	13.9	27.0	37.4	52.3
13	Pt RTD	79.0	80.6	80.9	81.9	82.2
14	Pt RTD	79.1	82.0	82.9	83.6	83.6
15	Pt RTD	79.1	82.7	82.9	83.5	83.5
16	Pt RTD	80.0	80.1	80.0	80.3	80.2
17	Pt RTD	80.0	OPEN	OPEN	OPEN	OPEN
18	Pt RTD	80.8	91.5	91.5	92.5	92.5
19	Cu/CON Te	200.0	182.5	182.8	188.6	188.9
20	Cu/CON Te	200.0	183.1	183.6	189.2	189.5
21	Cu/CON Te	299.7	286.2	287.7	296.9	297.5
22	Cu/CON Te	300.0	290.8	292.5	302.0	302.6
23	Cu/CON Te	300.0	291.2	292.8	302.3	302.9

The CCS temperature stations at 20 K and 80 K are used to structurally support the thermal radiation shields. Copper cable straps are used to heat sink each CCS temperature station to the shield that it supports, thereby employing the CCS temperature station to function as a heat intercept at the shield temperature. Figure 4a features HLTF measurements on a 5x7 CCS, and shows the temperature profile along an 80 K heat intercept heat sink strap. Figure 4b shows measurements made in the SSC thermal model, and profiles the 5x7 CCS temperatures along a 20 K heat intercept heat sink strap.

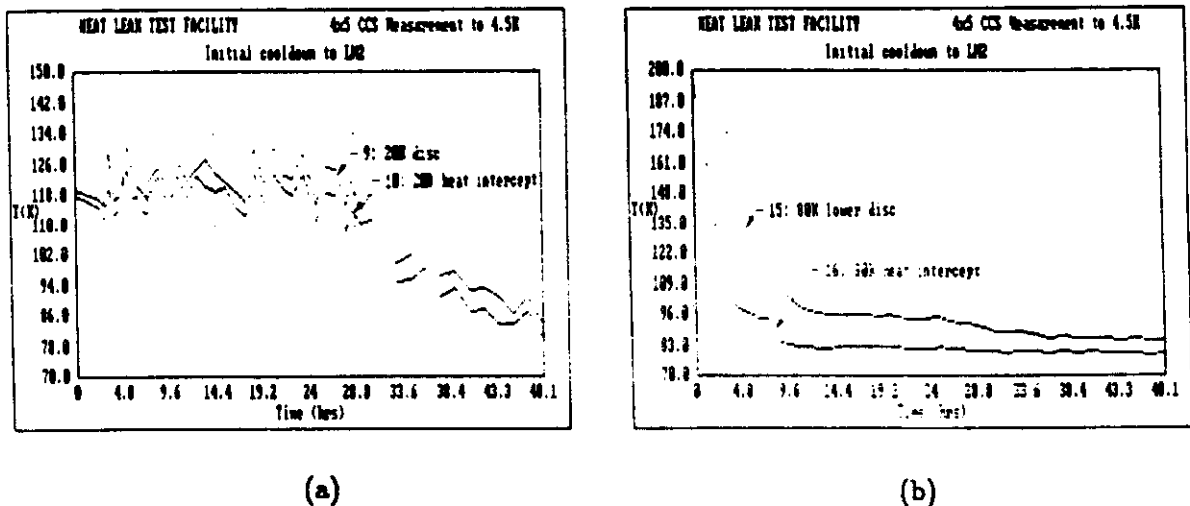


Fig. 3. 4x5 CCS component temperatures during thermal cycle. (a) at 20 K intercept, (b) at 80 K intercept.

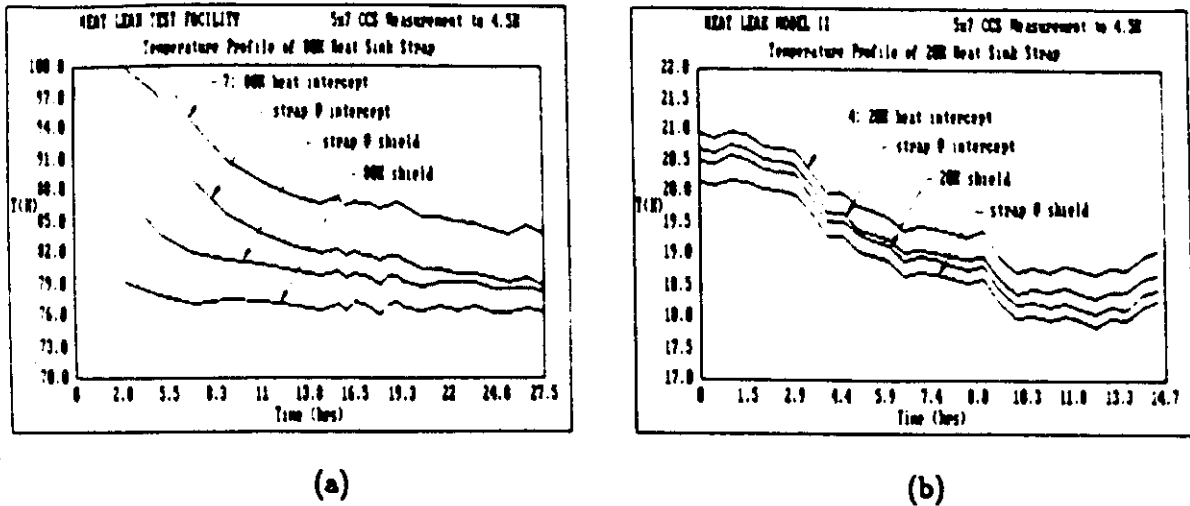


Fig. 4. 5x7 CCS temperature profile of heat sink straps.
 (a) at 80 K heat sink strap (b) at 20 K heat sink strap.

5x7 CCS TEST INSTRUMENTATION AND THERMAL PERFORMANCE RESULTS

Thermal performance measurements of the 5x7 CCS in the HLTF used the test geometry as shown in Fig. 2. Carbon resistors and platinum RTDs provided the temperature sensor instrumentation along the conductive heat path.

In an experimental test arrangement separate from that of the HLTF, the thermal performance of the 5x7 CCS was also evaluated. A full length SSC dipole magnet thermal model (SSC-TM) was constructed and its thermal performance evaluated.⁹ The thermal model is identical to magnet models except that the cold mass contains a simulated coil assembly. In the thermal model, (see Fig. 5) the cold mass and shields are supported relative to the vacuum vessel at five points along their lengths with each 5x7 CCS supporting a structural load of approximately 1455 kg. Temperature measurements along the 5x7 CCS were limited to the metal rings at the CCS temperature stations.

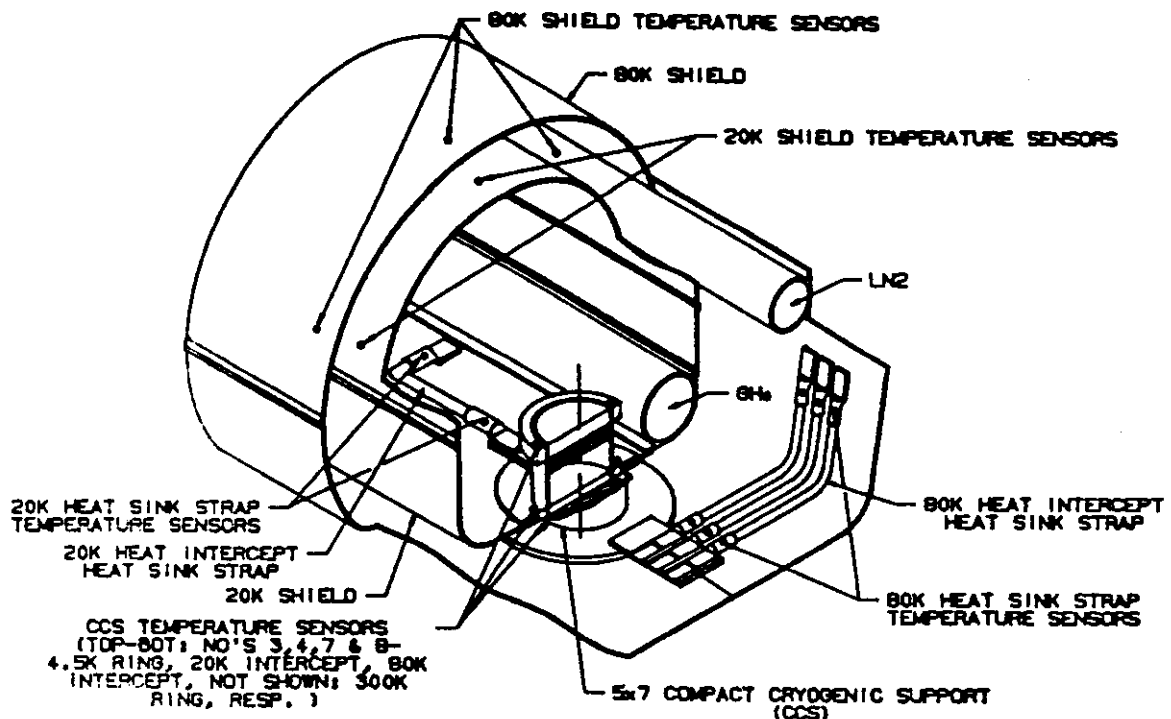
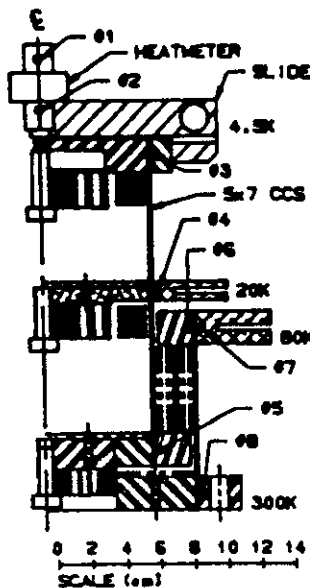


Fig. 5. 5x7 CCS installation in a full length SSC dipole magnet thermal model.

Table 2. 5x7 CCS Thermal Performance Results From The HLTF And SSC-TM



5x7 CCS TEMPERATURE PROFILE MEASUREMENTS (K) IN THE HEAT LEAK FACILITY AND SSC THERMAL MODEL									
SENSOR NUMBER	DESIGN TEMP. (K)	10K HEAT INTERCEPT		20K HEAT INTERCEPT		30K HEAT INTERCEPT		30K HEAT INTERCEPT	
		HLTF	SSC-TM	HLTF	SSC-TM	HLTF	SSC-TM	HLTF	SSC-TM
1	4.5	4.8	-	5.1	-	5.5	-	5.5	-
2	-	5.5	-	6.5	-	7.2	-	7.7	-
3	4.5	7.8	6.6	12.3	9.2	14.3	10.7	15.8	11.8
4	10.0	11.4	12.2	-	-	-	-	-	-
	20.0	-	-	22.7	22.8	-	-	-	-
	30.0	-	-	-	-	28.6	29.4	-	-
	36.0	-	-	-	-	-	-	33.3	34.6
5	79.1	84.2	-	84.8	-	84.7	-	85.8	-
6	80.0	80.0	-	80.7	-	80.4	-	81.4	-
7	80.0	83.1	83.6	83.7	84.7	83.3	84.0	84.3	84.2
8	300.0	296.8	293.6	296.2	298.1	296.1	290.5	295.1	297.6
HEAT LEAK MEASUREMENTS (mW) BY HEATMETER & MATERIAL PROPERTIES									
GM		5.5	-	10.6	-	27.8	-	34.3	-
G3		4.7	7.2	17.8	22.7	26.7	33.8	34.5	43.5
G4		139.1	137.2	112.3	108.9	93.2	86.5	79.9	68.2
G7		1077.1	1121.6	1048.0	1028.3	1094.8	1123.2	1089.0	1110.5

The thermal performance results of the 5x7 CCS obtained in the two facilities are compared in Table 2. Shown in Table 2 are temperature profile and heat leak measurements with the CCS at similar thermal conditions in the two facilities. In the HLTF, heat leak values to 4.5 K were obtained by direct measurement using the heatmeter as well as by calculation using the measured temperature profiles and the material properties for G-11CR thermal conductivity. Heat leak values to the remaining CCS temperature stations were derived using only the temperature profiles and material properties. In the thermal model, the heat leak values to the CCS temperature stations were derived by temperature and material properties alone.

DISCUSSION

The fabric reinforcement in G-11CR is a plain weave E-glass cloth having interlaced threads in the warp (length) and fill (width) directions of 43 threads per inch (16.9 per centimeter) and 32 threads per inch (12.6 per centimeter), respectively. Tubular G-11CR has the warp threads wrapped circumferentially about the tube and the fill threads along the tube length. Normal to the fabric weave is along tube radii. The CCS conductive heat path is along the tube length and is therefore in the fill direction.

G-11CR thermal conductivity (κ) values are reported by Kasen et al.¹⁰ for the warp, and normal to the fabric weave directions; however, little published data could be found for thermal conductivity for the fill direction. Equation 1 was used with the referenced measurements of warp and normal thermal conductivity to derive values for thermal conductivity for the fill direction.

$$\kappa_{\text{fill}} = \kappa_{\text{warp}} - \left((1 - 32/43) (\kappa_{\text{warp}} - \kappa_{\text{normal}}) \right) \quad (1)$$

Thermal impedance is offered by the CCS cold mass slide connection, and is realized as a reduction to the CCS conductive heat leak. This fact is made apparent by the steady-state temperature level above 4.5 K at which the CCS connection to the cold mass slide equilibrates. Calculations show a heat leak reduction of 33% under the 273 kg load in the HLTF, and an 18% reduction under the 1455 kg load in the SSC-TM.

CONCLUSIONS

- Supports can be designed, built, and operated as required by the SSC.
- The CCS shrink fit design assumption that the clamping force in a CCS shrink fitted junction is nearly constant for junction thermal excursions has been verified by the tracking of the junction components temperatures.
- Temperature profile and heat leak measurements in the Heat Leak Test Facility and in the SSC thermal model compare very favorably; differences are largest in the measurements to 4.5 K (lower temperatures yielding higher heat leak values) and can be attributed to better mechanical and thermal contact due to higher loading in the thermal model than in the HLTF (1455 kg vs 273 kg, respectively).
- The cold mass slide connection presents a thermal impedance along the conduction heat path of the CCS. The result is a lower heat leak to 4.5 K.
- Heat leak measurements to 4.5 K in the HLTF by the heatmeter agree closely with calculated values using the measured temperatures and material thermal properties, and agree well with design values.

ACKNOWLEDGEMENTS

The authors express our sincere appreciation to Messrs. Ray Hanft, Moyses Kuchnir, Peter Limon, Paul Mantsch, Peter Mazur and Mike McAshan for their dedicated interest, time, criticism and constructive evaluation of these measurements and methods.

The work as presented was performed at Fermi National Accelerator Laboratory which is operated by Universities Research Association Inc., under contract with the U.S. Department of Energy.

REFERENCES

1. R.C. Niemann et al., The cryostat for the 6 T magnet option, in: "Advances in Cryogenic Engineering" Vol. 31, Plenum Press, New York (1986), p. 63.
2. T.H. Nicol, R.C. Niemann and J.D. Gonczy, A suspension system for superconducting super collider magnets, in: "Proc. Eleventh Intl. Cryo. Conf.," Butterworth, Guilford, UK (1986), p.533.
3. T.H. Nicol, R.C. Niemann and J.D. Gonczy, SSC magnet cryostat suspension system design and performance, in: "Advances in Cryogenic Engineering," Vol. 33, Plenum Press, New York (to be published).
4. J.D. Gonczy et al., Heat leak measurement facility, in: "Advances in Cryogenic Engineering" Vol. 31, Plenum Press, New York (1986), p. 1291.
5. M. Kuchnir, Pulsed current resistance thermometry, in: "Advances in Cryogenic Engineering" Vol. 29, Plenum Press, New York (1984), p. 879.
6. E.T. Larson et al., Improved design for a SSC coil assembly suspension connection, in: "Advances in Cryogenic Engineering," Vol. 33, Plenum Press, New York (to be published).
7. M. Kuchnir, J.D. Gonczy and J.L. Tague, Measuring heat leak with a heatmeter, in: "Advances in Cryogenic Engineering," Vol. 31, Plenum Press, New York (1986), p. 1285.
8. R.C. Niemann et al., The cryostat for the SSC 6 T magnet option, in: "Advances in Cryogenic Engineering," Vol. 31, Plenum Press, New York (1986), p. 63.
9. R.C. Niemann et al., SSC dipole magnet cryostat thermal model measurement results, in: "Advances in Cryogenic Engineering," Vol. 33, Plenum Press, New York (to be published).
10. M.B. Kasen et al., Mechanical, electrical, and thermal characterization of G-10CR and G-11CR glass-cloth/epoxy laminates between room temperature and 4 K, in: "Advances in Cryogenic Engineering Materials," Vol. 26, Plenum Press, New York (1979), p. 235.